Higher harmonics increase LISA's mass reach for supermassive black holes

Bala R Iyer

Raman Research Institute
Bangalore

In collaboration with K.G. Arun, B.S. Sathyaprakash and Siddhartha Sinha

IAP, 2007

Supermassive black holes

Strong observational evidence for the existence of supermassive black holes (SMBHs) with masses in the range of $10^6 M_\odot$–$10^9 M_\odot$ in most galactic nuclei

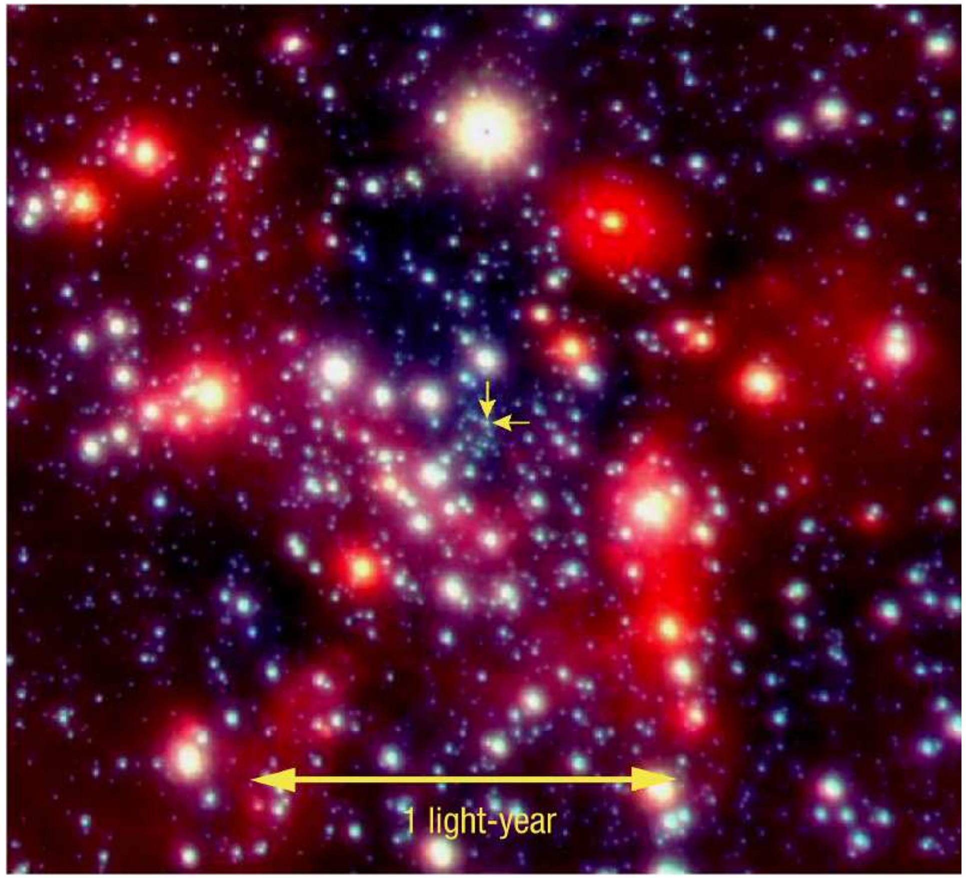

The Centre of the Milky Way
(VLT YEPUN + NACO)

ESO PR Photo 23a/02 (9 October 2002)

Supermassive black hole binaries

Mergers of galaxies, as evidenced by high-redshift surveys, should give rise to binaries containing SMBHs

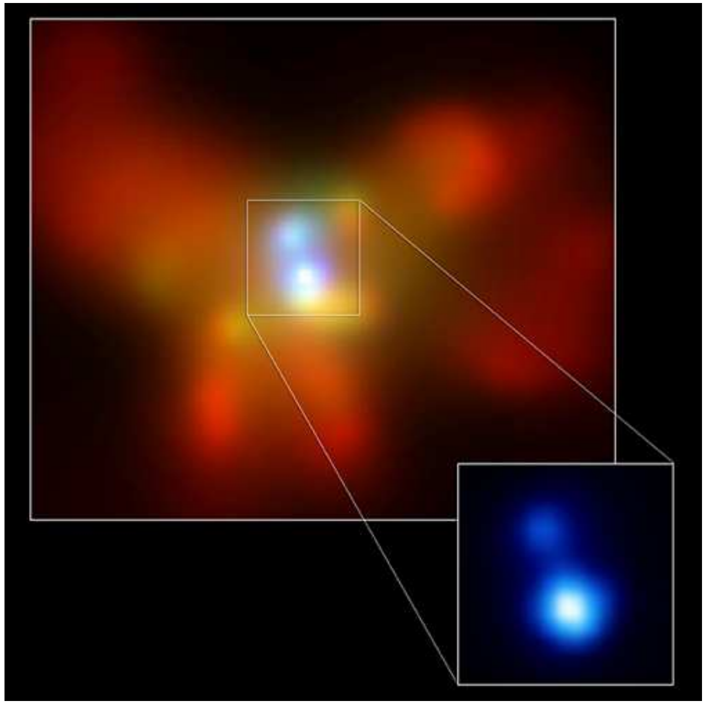

Late stage evolution of a SMBH binary is dictated by the emission of GW..
Leads to coalescence of the two holes...
X-ray observations have revealed the existence of at least one such system that would coalesce within the Hubble time (NGC 6240)

Supermassive black hole binaries and LISA

Emitted GW could be detected by the planned Laser Interferometer Space Antenna (LISA)

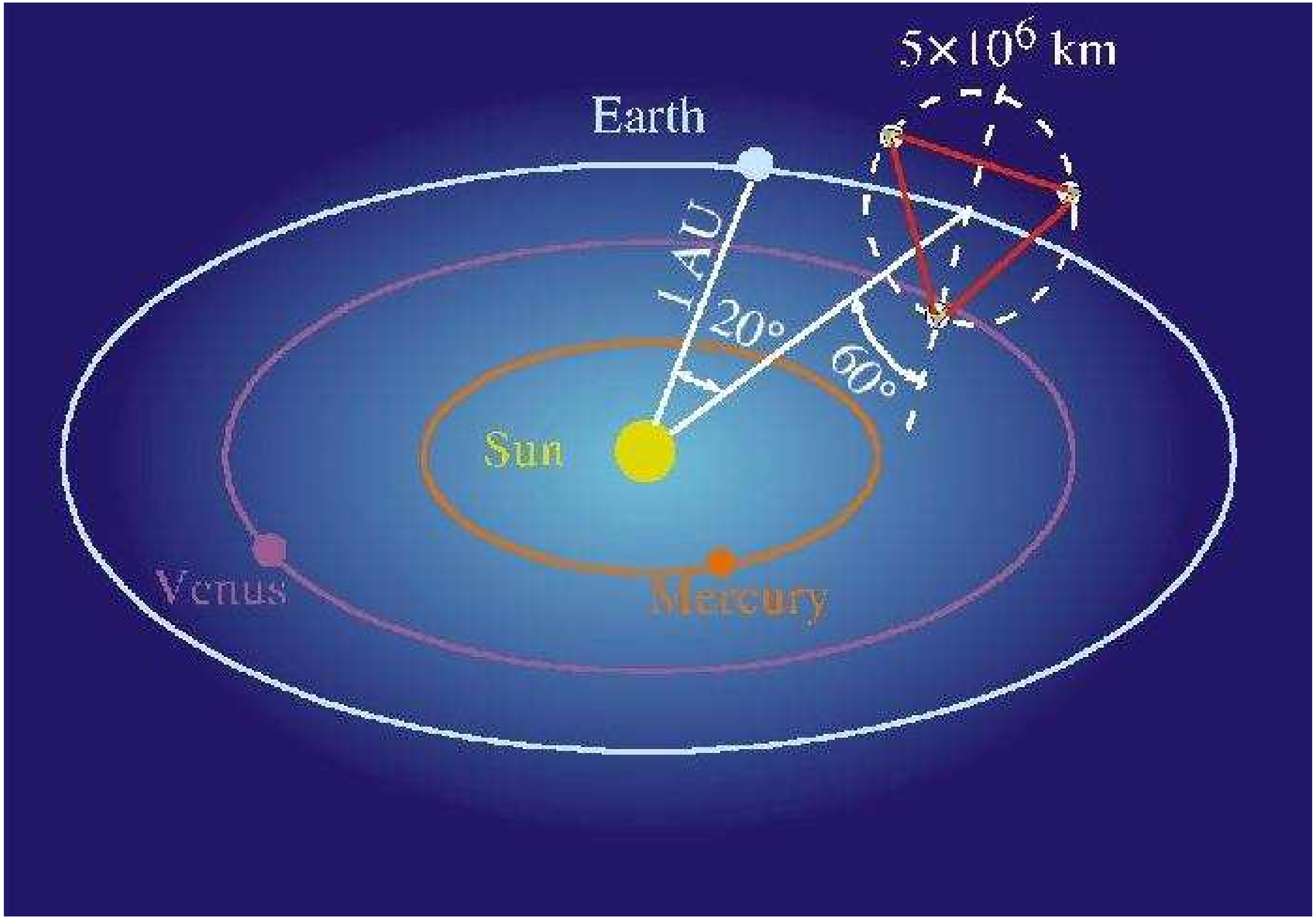

LISA Features..

- LISA will be sensitive to GW in a lower frequency band ($10^{-4} - 10^{-1}$Hz) unobservable by any ground-based detector due to seismic noise. Terrestrial interferometers are high frequency detectors ($10^{1} - 10^{3}$Hz)
- The ($10^{-4} - 10^{-1}$Hz) band contains many known GW sources that LISA is 'guaranteed' to see -
  Short-period binary star systems, Stochastic GW background from EU, Inspiral of compact stellar mass objects into SMBH, Merger of two SMBH's
- LISA and ground-based interferometers also differ in regard to how they identify the angular position of the source on the sky
- Network of three ground-based detectors, will be able to determine the source position to within $\sim 1^o$ by a standard time-of-flight method ($\lambda_{\rm GW} << D$ (distance between detectors))
- LISA: Not a network of detectors..
  $\lambda_{\rm GW}$ in the heart of the LISA band ($\sim 10^{-3}$ Hz) is of order 1 AU ..
- LISA: Two detectors, each measuring a different polarization of GW.
  Data: Two time series.
  All info about source position and *all other* physical variables must be extracted from these two time series.

Angular Resolution: LISA

Cutler PRD 57, 7089, 1998

- Angular position info encoded in the time series in the following ways.
  1. Relative amplitudes and phases of the two polarizations provide some position information.
  2. Most sources will be 'visible' to LISA for months or longer.
     LISA's translational motion around the Sun imposes on the signal a periodic Doppler shift, whose magnitude and phase depend on the angular position of the source.
     (Analog: Doppler shift due to the Earth's rotation used to determine a pulsar's position in radio astronomy)
  3. LISA's orientation rotates on a one-year timescale
     Causes a further source-position-dependent modulation on the measured signal

Click here to view the movie

LISA Annual Orbit

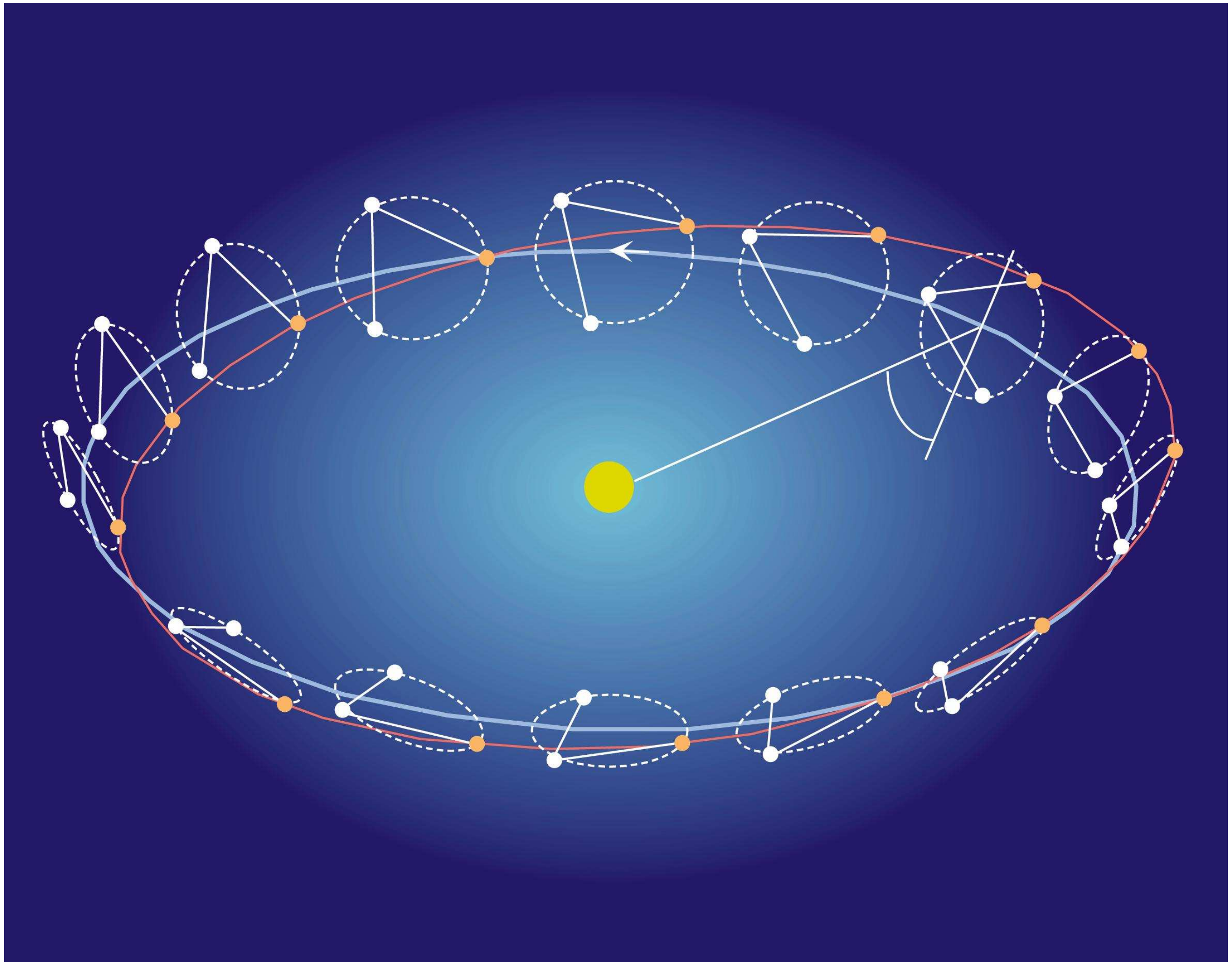

Angular Resolution: LISA

- Effect of the detector's changing orientation on a monochromatic signal of frequency f_0 is to spread the measured power over (roughly) a range $f_0 \pm 2/T$, where T is one year.
- Effect of the periodic Doppler shift coming from the detector's center-of-mass motion is to spread the power over a range $f_0(1 \pm v/c)$, where $v/c \sim 10^{-4}$.
- Two effects are therefore of roughly equal size at $f_0 \sim 10^{-3}\,\mathrm{Hz}$, near the center of the LISA band. Rotational modulation more significant at lower frequencies; Doppler modulation is more significant at higher frequencies.
- Uncertainty in position measurement arises since one must extract *all* the physical parameters of the binary: orbital plane, masses of the bodies, etc from this pair of time series. Errors in determining the source position correlated with errors in these other parameters.
- LISA's angular resolution significantly worse than if one ignored these correlations. LISA's angular resolution depends not just on the detector and SNR but on the type of source as well

LISA Science Goals..

- Observation of SMBH binaries at high redshifts is one of the major science goals of LISA.
- Striking feature of the mergers is the 'huge' amplitude of the emitted GW.
- LISA capable of detecting SMBH mergers at redshift ($z < 10$, say) with SNR $\sim 10^3$, for BH in the mass range $10^4 M_\odot < M(1+z) < 10^7 M_\odot$.
- Event rate for such mergers is highly uncertain (Several per year, or $<< 1$/yr)
- If SMBH mergers *were* discovered, provide a way of determining all the basic cosmological parameters – H_0, Ω_0, and Λ_0 – to remarkably high accuracy.
- From GWF expects to determine luminosity distance D_L to the source to an accuracy of roughly $(S/N)^{-1}$.
- If source position on the sky could be determined to sufficient accuracy that one could identify the host galaxy or galaxy cluster, presumably one could also determine the redshift optically.
- A mere handful of such measurements would be sufficient to determine H_0, Ω_0, and Λ_0 to roughly 1% accuracy.

LISA Science Goals..

- Observations will allow us to probe the evolution of SMBHs and structure formation
- Provide an unique opportunity to test General Relativity (and its alternatives) in the strong gravity regime
- Does LISA has sufficient angular resolution to make such identifications possible? Cutler PRD **57**, 7089 (1998)
- Found that LISA does roughly a factor 10 worse than expected: typically $\Delta D_L/D_L \sim 1\%$;
- LISA will determine the SMBH location to no better than $\sim 10^{-5}$ steradians (and typically to $\sim 10^{-4}$ steradians)
  Not sufficient by itself to permit identification of the host galaxy.
- However position measurement will be available days before the final merger; other telescopes (radio, optical, X-ray) should know when and where to look, so if the merger is accompanied by an electromagnetic outburst host galaxy might still be determined.

Chirp Signal, Matched Filtering

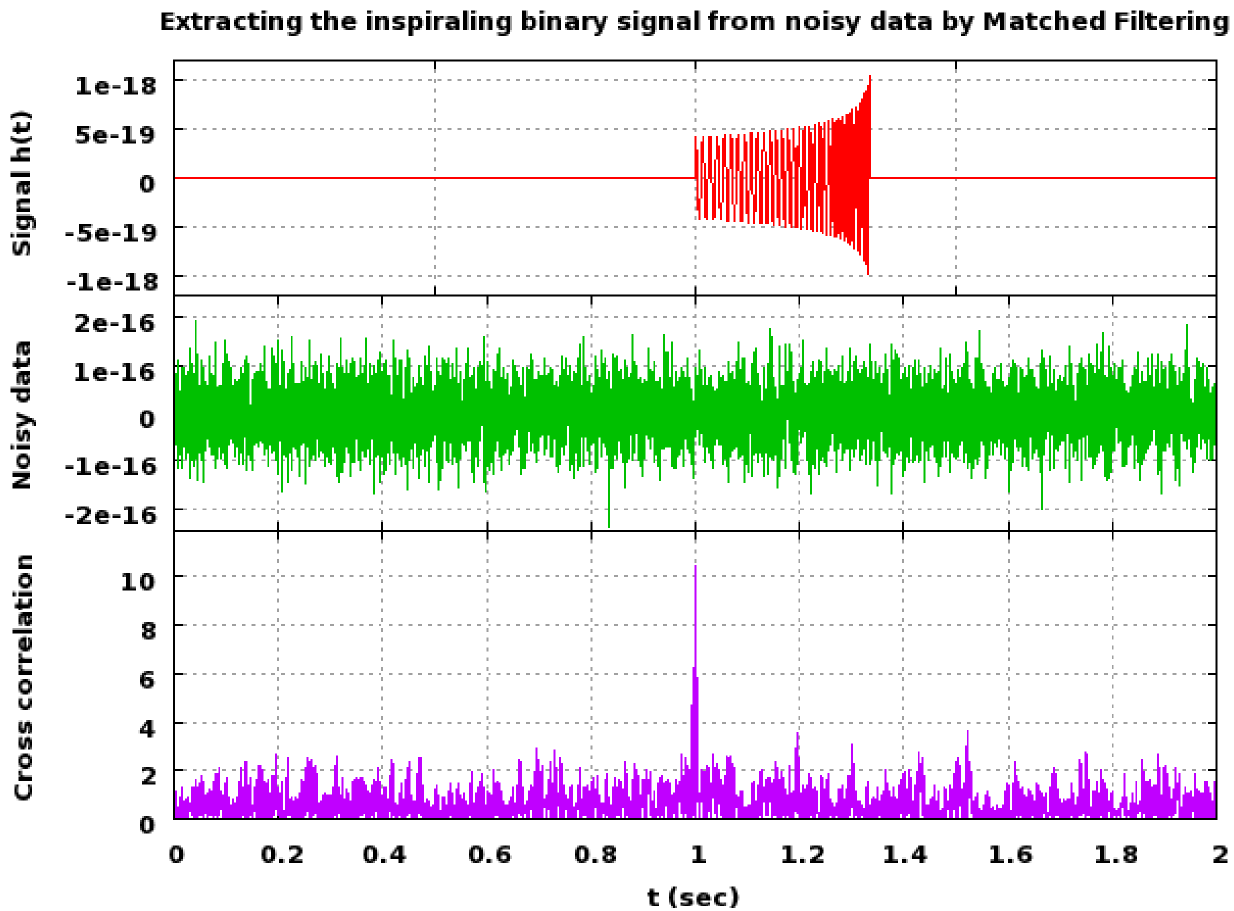

From Anand Sengupta (IUCAA)

GW polarisations - 2.5PN Full waveform

(Arun,Blanchet,BRI, Qusailah,2004)

$$x = \left(\frac{Gm\omega_{\mathrm{orb}}}{c^3} \right)^{2/3}$$

$$h(t) = F_+ h_+(t) + F_\times h_\times(t).$$

$$h_{+,\times}(t) = \frac{2G\mu}{c^2 R} \; x(t) \quad \times \{ H^{(0)}_{+,\times}(t) + x^{1/2}(t) H^{(1/2)}_{+,\times}(t) + \cdots + x^{5/2}(t) H^{(5/2)}_{+,\times}(t) \}$$

$$H^{(0)}_+ = -(1 + c_i^2) \cos 2\Psi(t),$$

$$H^{(0)}_\times = -2c_i \sin 2\Psi(t), \cdots$$

$$\begin{aligned} F_+(\theta,\phi,\psi) &= \frac{1}{2}\left(1+\cos^2(\theta)\right)\cos(2\phi)\cos(2\psi) - \cos(\theta)\sin(2\phi)\sin(2\psi), \\ F_\times(\theta,\phi,\psi) &= \frac{1}{2}\left(1+\cos^2(\theta)\right)\cos(2\phi)\sin(2\psi) + \cos(\theta)\sin(2\phi)\cos(2\psi). \end{aligned}$$

3.5PN phasing - $\phi(t)$

(Blanchet, Faye, BRI, Joguet 2002; Blanchet, Damour, Esposito-Farèse, BRI 2004)

$$
\begin{aligned}
\Psi &= -\frac{1}{\nu}\Bigg\{\tau^{\frac{5}{8}} + \left(\frac{3715}{8064}+\frac{55}{96}\nu\right)\tau^{\frac{3}{8}} - \frac{3}{4}\pi\tau^{\frac{1}{4}} \\
&+ \left(\frac{9275495}{14450688}+\frac{284875}{258048}\nu+\frac{1855}{2048}\nu^2\right)\tau^{\frac{1}{8}} \\
&+ \left(-\frac{38645}{172032}-\frac{15}{2048}\nu\right)\pi\ln\left(\frac{\tau}{\tau_0}\right) \\
&+ \left(\frac{831032450749357}{57682522275840}-\frac{53}{40}\pi^2-\frac{107}{56}C+\frac{107}{448}\ln\left(\frac{\tau}{256}\right)\right. \\
&+ \left[-\frac{123292747421}{4161798144}+\frac{2255}{2048}\pi^2+\frac{385}{48}\lambda-\frac{55}{16}\theta\right]\nu \\
&+ \left.\frac{154565}{1835008}\nu^2-\frac{1179625}{1769472}\nu^3\right)\tau^{\frac{-1}{8}} \\
&+ \left(\frac{188516689}{173408256}+\frac{140495}{114688}\nu-\frac{122659}{516096}\nu^2\right)\pi\tau^{\frac{-1}{4}}\Bigg\}.
\end{aligned}
$$

where, $\tau = \frac{\nu\, c^3\,(t_c - t)}{5\,G\,m}$, $C = 0.577..$

$$\theta = -\frac{11831}{9240};\ \hat{\theta} = \frac{1039}{4620};\ \lambda = -\frac{1987}{3080}$$

3.5PN phasing -$x(t)$

$$
\begin{aligned}
x \quad = \quad & \frac{1}{4}\tau^{-1/4}\Bigg\{1+\left(\frac{743}{4032}+\frac{11}{48}\nu\right)\tau^{-1/4}-\frac{1}{5}\pi\tau^{-3/8} \\
+ \quad & \left(\frac{19583}{254016}+\frac{24401}{193536}\nu+\frac{31}{288}\nu^2\right)\tau^{-1/2} \\
+ \quad & \left(-\frac{11891}{53760}+\frac{29}{1920}\nu\right)\pi\tau^{-5/8} \\
+ \quad & \Bigg\{\Bigg(-\frac{10052469856691}{6008596070400}+\frac{1}{6}\pi^2+\frac{107}{420}c-\frac{107}{3360}\ln\left(\frac{\tau}{256}\right) \\
+ \quad & \left[\frac{15335597827}{3901685760}-\frac{451}{3072}\pi^2-\frac{77}{72}\lambda+\frac{11}{24}\theta\right]\nu \\
- \quad & \frac{15211}{442368}\nu^2\frac{25565}{331776}\nu^3\Bigg)\tau^{-3/4}\Bigg\} \\
+ \quad & \left(-\frac{113868647}{433520640}-\frac{141389}{483840}\nu+\frac{275201}{3870720}\nu^2\right)\pi\tau^{-7/8}\Bigg\} \quad .
\end{aligned}
$$

2.5PN in Amplitude

$$
\begin{aligned}
H_{+}^{(0)} &= -(1+c_i^2)\cos 2\Psi - \frac{1}{96}\, s_i^2\,(17+c_i^2)\,, \\
H_{+}^{(0.5)} &= -\,s_i\,\frac{\delta m}{m}\left[\cos\Psi\left(\frac{5}{8}+\frac{1}{8}\,c_i^2\right)-\cos 3\Psi\left(\frac{9}{8}+\frac{9}{8}\,c_i^2\right)\right], \\
H_{+}^{(1)} &= \cos 2\Psi\left[\frac{19}{6}+\frac{3}{2}\,c_i^2-\frac{1}{3}\,c_i^4+\nu\left(-\frac{19}{6}+\frac{11}{6}\,c_i^2+c_i^4\right)\right] \\
&\quad -\cos 4\Psi\left[\frac{4}{3}\,s_i^2(1+c_i^2)(1-3\nu)\right],\ldots\ldots\ldots \\
H_{\times}^{(0)} &= -2c_i\sin 2\Psi\,, \\
H_{\times}^{(0.5)} &= s_i c_i\,\frac{\delta m}{m}\left[-\frac{3}{4}\sin\Psi+\frac{9}{4}\sin 3\Psi\right], \\
H_{\times}^{(1)} &= c_i\sin 2\Psi\left[\frac{17}{3}-\frac{4}{3}\,c_i^2+\nu\left(-\frac{13}{3}+4\,c_i^2\right)\right] \\
&\quad +c_i\,s_i^2\sin 4\Psi\left[-\frac{8}{3}(1-3\nu)\right],\ldots\ldots\ldots
\end{aligned}
$$

$$c_i \equiv \cos i\,;\; s_i \equiv \sin i$$

2.5PN in Amplitude

$$
\begin{aligned}
H_+^{(2.5)} \quad = \quad & s_i \frac{\delta m}{m} \cos\Psi \left[\frac{37127}{107520} - \frac{4937}{15360} c_i^2 + \frac{217}{9216} c_i^4 - \frac{1}{9216} c_i^6 \right. \\
& + \nu \left(\frac{71537}{26880} + \frac{11}{1280} c_i^2 - \frac{35}{768} c_i^4 + \frac{1}{2304} c_i^6 \right) \\
& \left. + \nu^2 \left(-\frac{3451}{9216} + \frac{673}{3072} c_i^2 - \frac{5}{9216} c_i^4 - \frac{1}{3072} c_i^6 \right) \right] \\
& + \pi \cos 2\Psi \left[\frac{19}{3} + 3\, c_i^2 - \frac{2}{3} c_i^4 + \nu \left(-\frac{19}{3} + \frac{11}{3} c_i^2 + 2\, c_i^4 \right) \right] \\
& + s_i \frac{\delta m}{m} \cos 3\Psi \left[\frac{18261}{5120} - \frac{4941}{1024} c_i^2 - \frac{15309}{5120} c_i^4 + \frac{729}{5120} c_i^6 \right. \\
& + \nu \left(-\frac{24117}{1280} + \frac{6393}{1280} c_i^2 + \frac{7749}{1280} c_i^4 - \frac{729}{1280} c_i^6 \right) + \ldots\ldots\ldots\ldots \\
& + \cos 7\Psi [\ldots\ldots\ldots\ldots\ldots\ldots\ldots\ldots]
\end{aligned}
$$

Restricted Vs Full Waveforms

- Since matched filtering is more sensitive to the phase of the signal than its amplitude, search algorithms so far have deployed a waveform model involving only the *dominant harmonic* (at twice the orbital frequency), although the phase evolution itself is included to the maximum available post-Newtonian (PN) order (currently 3.5PN, for non-spinning systems)
- Waveforms in which all *amplitude* corrections are neglected, but the *phase* is treated to the maximum available order, are called *restricted waveforms* (RWF) and these are what are used so far in the analysis of data from ground-based detectors
- LISA is designed to detect GW in the frequency-band 0.1–$100\,\mathrm{mHz}$. This frequency range determines the range of masses accessible to LISA because the inspiral signal would end when the system's orbital frequency reaches the mass-dependent last stable orbit (LSO).
- In the test-mass approximation, the angular velocity $\omega_{\rm LSO}$ at LSO is given by $\omega_{\rm LSO} = 6^{-3/2} M^{-1}$, where M is the total mass of the binary.

Restricted Vs Full Waveforms

- Search templates that contain only the dominant harmonic cannot extract power in the signal beyond
  $f_{\rm LSO} = \omega_{\rm LSO}/\pi \simeq 4.39(M/10^6 M_\odot)^{-1}{\rm mHz}.$
  Frequency range $[0.1,\ 100]\ {\rm mHz}$ corresponds to mass range $\sim 4.39 \times [10^7,\ 10^4] M_\odot$ of binary black holes accessible to LISA
- However, there is observational evidence for the existence of many SMBHs whose masses are of the order of 10^8–$10^9 M_\odot$.
- LISA will be *unable* to observe binaries containing SMBHs in this mass range if search templates waveforms contain *only* the dominant harmonic.
- In this work we consider the advantage of using the *full wave forms* (FWF) in the context of LISA

Restricted Vs Full Waveforms

- Inclusion of higher-order amplitude terms in the waveform introduces the following two new features:
  1. appearance of higher harmonics of the orbital phase
  2. PN amplitude corrections to the leading as well as higher harmonics of the orbital frequency.
- The $(2n+2)^{\mathrm{th}}$ harmonic first appears at the n^{th} PN order in amplitude
- In expressions for the 'plus' and 'cross' polarizations, all odd harmonics of the orbital frequency are proportional to $\frac{\delta m}{M}$, where δm is the difference in the masses of the binary components.

RWF vs FWF - Ground Based Detectors

- For ground-based detectors, Van Den Broeck and Sengupta examined the implications of going beyond the restricted PN approximation and employing instead the full waveform
- The two main implications of the comprehensive analysis for terrestrial GW detectors may be summarized as follows:
  1. For binary neutron stars and stellar mass black holes, restricted waveforms over-estimate the SNR as compared the full waveform.
  2. The use of the full waveforms significantly increases the mass-reach of second and third generation detectors, advanced LIGO and Virgo being able to observe systems with total mass $\sim 400 M_\odot$ and a third generation detector as high as $10^3 M_\odot$.

RWF vs FWF - LISA

- We study in the context of LISA the implication of using templates based on the FWF (i.e. including *all* known harmonics of the orbital phase and *all* known amplitude corrections in the GW polarisations).
- Coalescences of SMBH binaries with masses $\sim 10^{8-9} M_\odot$ will *not* be observable by LISA if one uses only templates based on the RWF.
- Using templates based on amplitude corrected full waveforms, instead of the usual restricted waveforms, will enable LISA to observe coalescences of SMBH binaries with total mass $\sim 10^8 M_\odot$ $(10^9 M_\odot)$ if the lower frequency cut-off LISA can achieve is $\sim 10^{-4}$Hz $(10^{-5}$Hz).

Amplitude corrected waveform

- Waveform $h(t)$ is a linear combination of sine and cosine functions of multiples of the orbital phase $\Psi(t)$.
  2.5PN polarization contains the first seven harmonics of the orbital phase, the dominant harmonic being the one at twice the orbital phase.
- Signal depends on the parameters:
  D_L, the luminosity distance to the binary,
  m the total (red-shifted) mass,
  ν the symmetric mass-ratio (reduced mass divided by total mass),
  the spherical polar angles (θ, ϕ) determining the direction of the "line-of-sight",
  inclination angle ι of the angular momentum $\mathbf{L}$ of the binary wrt the line-of-sight,
  polarization angle ψ - orientation of the projection of $\mathbf{L}$ in the plane normal to the line-of-sight.

Amplitude corrected waveform

- Rewrite the waveform in terms of only cosines

$$h(t) = \frac{2M\nu}{D_L} \sum_{k=1}^{7} \sum_{n=0}^{5} A_{(k,n/2)} \cos[k\Psi(t) + \phi_{(k,n/2)}]\, x^{\frac{n}{2}+1}(t),$$

  Coefficients $A_{(k,n/2)}$ and $\phi_{(k,n/2)}$ are functions of $(\nu, \theta, \phi, \psi, \imath)$
  $x(t) = (2\pi M F(t))^{2/3}$ is the post-Newtonian parameter
  with $F(t)$ the instantaneous *orbital* frequency.

- $A_{(k,n/2)}$ - Polarization amplitude
  $\frac{2M\nu}{D_L} x^{n/2+1}(t)\, A_{(k,n/2)}$ - Wave amplitude
  $\phi_{(k,n/2)}$ - Polarization phase,
  corresponding to the $k^{\rm th}$ harmonic and $(n/2)^{\rm th}$ PN order.

- Orbital phase $\Psi(t)$: PN series in x, known to 3.5PN order

- For a non-spinning source and a detector whose position and orientation are almost constant during the time of observation of the signal, all the above mentioned angles are constants. e.g. Ground-based GW detectors

Amplitude corrected waveform - Time Domain

Modulations due to LISA's orbital motion

- LISA will be able to observe many sources from their early stages of inspiral.
  Most would last for a long time.
  Consider binary sources that last for a year or less before merger.
- LISA plane is tilted by 60° wrt plane of the ecliptic.
  During the course of its heliocentric orbit its orientation and position varies periodically, with a period of one year.
- Signal will suffer additional amplitude and phase modulations.
  Generalising Cutler (1998) from RWF to FWF,
  the signal as seen in LISA is of the form,

$$h(t) = \frac{\sqrt{3}}{2}\,\frac{2M\nu}{D_L}\sum_{k=1}^{7}\sum_{n=0}^{5} A_{(k,n/2)}(t)\cos[k\Psi(t) + \phi_{(k,n/2)}(t) + k\phi_D(t)]\, x^{\frac{n}{2}+1}(t)\,.$$

PN parameter $x(t)$ is still $(2\pi M F(t))^{2/3}$, but $F(t)$, is the orbital frequency as measured by a *non-rotating observer located at the solar-system barycentre*.

Amplitude corrected waveform - Time Domain

- $\phi_D(t)$ is the *Doppler phase*, accounting for the phase difference of the gravitational wave-front between LISA and the solar-system barycentre.
- Time-dependence of $\phi_D(t)$ is due to the orbital motion of LISA about the barycentre

$$\phi_D(t) = 2\,\pi\,F(t)\,R\,\sin\theta_S\,\cos[\phi(t) - \phi_S],$$

$R = 1$ AU,
Location: $(\theta_S,\,\phi_S)$, spherical polar angles of the direction to the source wrt the non-rotating observer at the solar-system barycentre,
$\phi(t)$, the angular position of LISA wrt barycentre given by $\phi(t) = 2\,\pi\,\frac{t}{T}$,
T being equal to one year.
Orientation: $(\theta_L,\,\phi_L)$, spherical polar angles determining direction of orbital angular momentum of the binary
Discuss and Transform carefully from Fixed barycenter to roating LISA (Cutler 1998)

Amplitude corrected WF - Frequency Domain

- Waveform valid in the adiabatic regime, where RR time-scale is much larger than the orbital time-scale
- Additional Amplitude and Doppler modulations in the waveform for LISA vary on time-scales of 1 yr (i.e. $\sim 3 \times 10^7\,\mathrm{s}$), while LISA can observe orbital periods at most up to $2 \times 10^5\,\mathrm{s}$, (i.e. GW frequencies of order $10^{-5}\,\mathrm{Hz.}$).
- Doppler modulations change much more slowly (a hundredth) than the orbital phase.
- Permits use of stationary phase approximation (SPA). Analytical form for the Fourier transform (FT) $\tilde{h}(f)$ of the signal:

$$\tilde{h}(f) \simeq \frac{\sqrt{3}}{2} \frac{2M\nu}{D_L} \sum_{k=1}^{7} \sum_{n=0}^{5} \frac{A_{(k,n/2)}(t(f/k))\, x^{\frac{n}{2}+1}(t(f/k))\, e^{-i\phi_{(k,n/2)}(t(f/k))}}{2\sqrt{k\dot{F}(t(f/k))}} \exp\left[i\,\psi(t(f/\right.$$

Over dot - derivative wrt time

$$\psi(t(f/k)) = 2\pi f\, t(f/k) - k\,\Psi(t(f/k)) - k\,\phi_D(t(f/k)) - \pi/4.$$

PN expansions for $t(F), \Psi(F), \dot{F}(F)$ are known.

Amplitude corrected WF - Frequency Domain

- $\dot{F}$ may be treated in different ways that could lead to numerically different results. In a numerical treatment, one could avoid performing a further re-expansion. Or, one could re-expand the denominator in the amplitude and truncate the resulting expression at the $n^{\rm th}$ PN order
  We follow the latter in this work.
- RR results in an increase in the orbital frequency $F(t)$ which will ultimately drive the system beyond the adiabatic inspiral phase and the inspiral waveform given above will no longer be valid.
- In the first approximation this is expected to occur when the orbital frequency $F(t)$ reaches $F_{\rm LSO}$ – the orbital frequency of the LSO of a Schwarzschild solution with the same mass as the binary's total mass M,

$$F_{\rm LSO} = (2\,\pi\,6^{\frac{3}{2}}\,M)^{-1}.$$

- Truncate the signal in the time domain at a time $t_{\rm LSO}$, given implicitly by $F(t_{\rm LSO}) = F_{\rm LSO}$.

Amplitude corrected WF - Frequency Domain

- In the SPA, the main contribution to the FT of the $k^{\rm th}$ harmonic at a given Fourier frequency f, comes from the neighbourhood of the time when the instantaneous value of the $k^{\rm th}$ harmonic sweeps past f.
  Thus the $k^{\rm th}$ harmonic is not expected to contribute significant power to the FT for frequencies above $k\,F_{\rm LSO}$, if the signal is truncated in the time domain beyond $t_{\rm LSO}$.
- Motivates truncation of the FT due to the $k^{\rm th}$ harmonic at frequencies above $k\,F_{\rm LSO}$ by a step function $\theta(k\,F_{\rm LSO} - f)$
  $\theta(x) = 1,\ x \geq 0;\ \theta(x) = 0,\ x < 0$

Choice of frequency cutoffs $\mathbf{f}_{\rm end}, \mathbf{f}_{\rm s}$

- Upper limit of integration $f_{\rm end}$ is taken to be the minimum of $7\,F_{\rm LSO}$ and 1 Hz (conventional upper cut-off for the LISA noise curve)
- Lower limit $f_{\rm s}$ chosen assuming LISA observes the inspiral for a duration $\Delta t_{\rm obs}$ before it reaches the LSO
- $k^{\rm th}$ harmonic will have a frequency $k\,F_{\rm in}$, $\Delta t_{\rm obs}$ before $t_{\rm LSO}$.
- Lower cut-off for the $k^{\rm th}$ harmonic should be the maximum of the lower cut-off of LISA (10^{-4} Hz) and $k\,F_{\rm in}$ and simply implemented by truncating the waveform due to the kth harmonic by another step-function $\theta(f - k\,F_{\rm in})$ and choosing $f_{\rm s}$ to be 10^{-4}Hz.
- $k^{\rm th}$ harmonic probes a larger interval of the frequency domain i.e. $k(F_{\rm LSO} - F_{\rm in})$ relative to the fundamental harmonic.
  We refer to this as the span of the $k^{\rm th}$ harmonic.

Choice of frequency cutoffs $\mathbf{f}_{\rm end}, \mathbf{f}_{\rm s}$

- Caveat with regard to the use of higher harmonics that is worth mentioning: In TD the WF should begin when the highest harmonic reaches the lower cutoff. For data analysis templates will be an order-of-magnitude longer than before. Sensible to use higher harmonics only in the case of higher masses
- Take $\Delta t_{\rm obs}$ to be one year. Specify the location of the source on the sky by the angles θ_S and ϕ_S. The orientation is given by the angles θ_L and ϕ_L, the spherical polar angles determining the direction of the orbital angular momentum $\mathbf{L}$ of the binary.
- Transformation between the fixed set of angles (θ_S, ϕ_S, θ_L, ϕ_L) and the time-dependent angular coordinates of the source $(\theta, \phi, \psi, \imath)$ as measured by LISA are given in Cutler 98.

SNR in LISA with higher harmonics

- Given a waveform h, the best signal-to-noise ratio (SNR) achieved using an optimal filter is given by

$$\rho[h] \equiv (h|h)^{1/2}$$

$(. | .)$ is the usual inner product in terms of the one-sided noise power spectral density $S_h(f)$ of the detector. With the FT convention,

$$\tilde{x}(f) = \int_{-\infty}^{\infty} x(t)\, \exp(-2\pi i f t)\, dt$$

the inner product is given by:

$$(x|y) \equiv 4 \int_{f_{\rm s}}^{f_{\rm end}} \frac{\mathrm{Re}[\tilde{x}^*(f)\tilde{y}(f)]}{S_h(f)} df.$$

For an optimal filter, which maximises the overlap of the signal with template

$$\rho^2 = 4 \int_{f_{\rm s}}^{f_{\rm end}} \frac{|\tilde{h}(f)|^2}{S_h(f)} df.$$

Use the non-sky-averaged noise-spectral-density Berti, Buonanno, Will

Observed signal spectrum with LISA

- Consider the SNR integrand, “noise-weighted signal power” per unit logarithmic frequency interval and Rewrite the SNR as

$$\rho^2 = 4\int_{f_s}^{f_{\rm end}} \frac{f\,|\tilde{h}(f)|^2}{S_h(f)} d\ln(f),$$

- Observed Spectrum $P(f)$ is

$$\mathcal{P}(f) \equiv \frac{d(\rho^2)}{d(\ln f)} = \frac{f\,|\tilde{h}(f)|^2}{S_h(f)},$$

- Observed spectrum is plotted versus frequency for given masses in Figures next

Observed Spectrum in LISA for $(10^5, 10^6)M_\odot$ binary

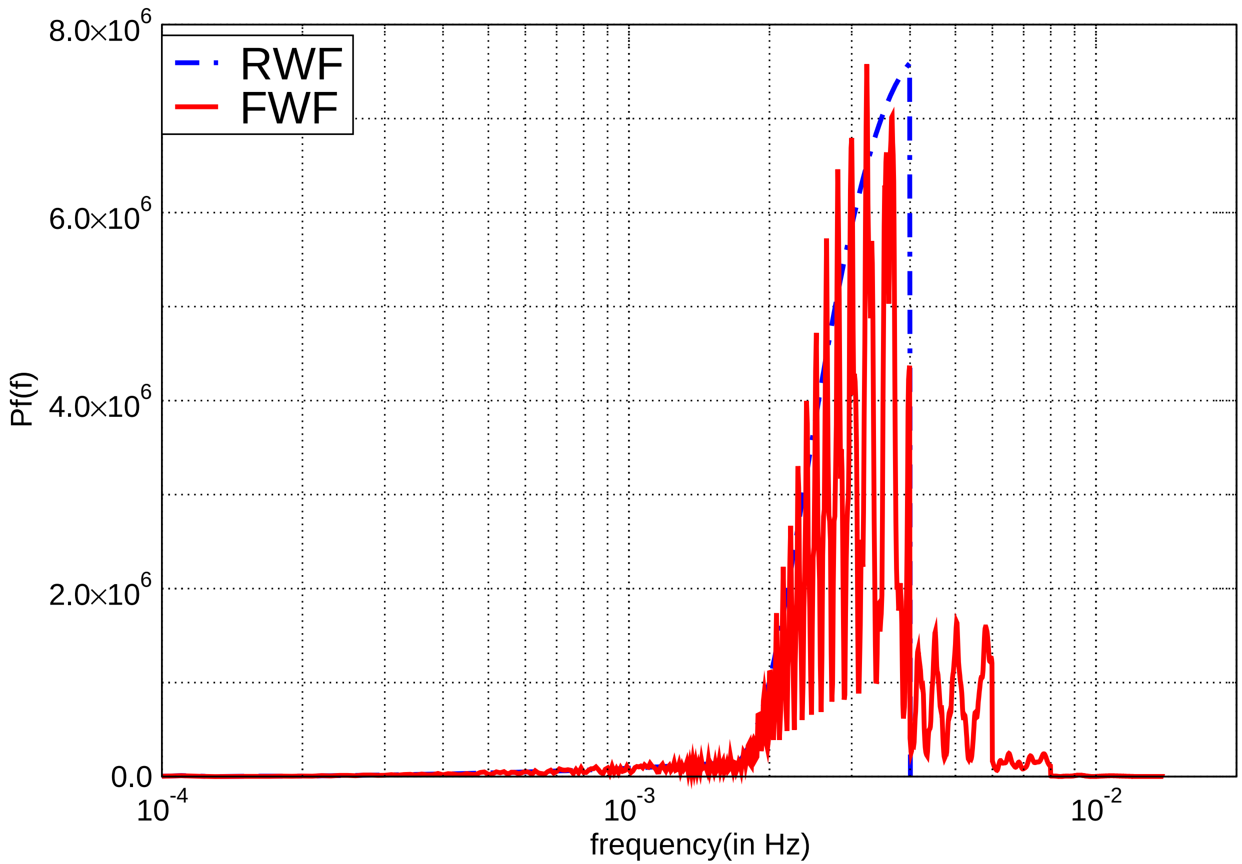

The source is assumed to be at 3 Gpc and its orientation wrt the solar-system barycentre is chosen to be $\theta_S = \cos^{-1}(-0.6)$, $\phi_S = 1$, $\theta_L = \cos^{-1}(0.2)$, $\phi_L = 3$. The spectrum is much more complicated and highly oscillatory for the FWF than for the RWF, because of interference between various harmonics. The higher frequency reach of the FWF is due to presence of higher harmonics. The spectrum for the system sharply rises at a frequency $\sim 2 \times 10^{-3}$Hz. Beyond this frequency, the effective LISA noise decreases sharply with increasing frequency leading to the observed increase in the spectrum.

Observed Spectrum in LISA - $2 \times (10^6, 10^7) M_\odot$

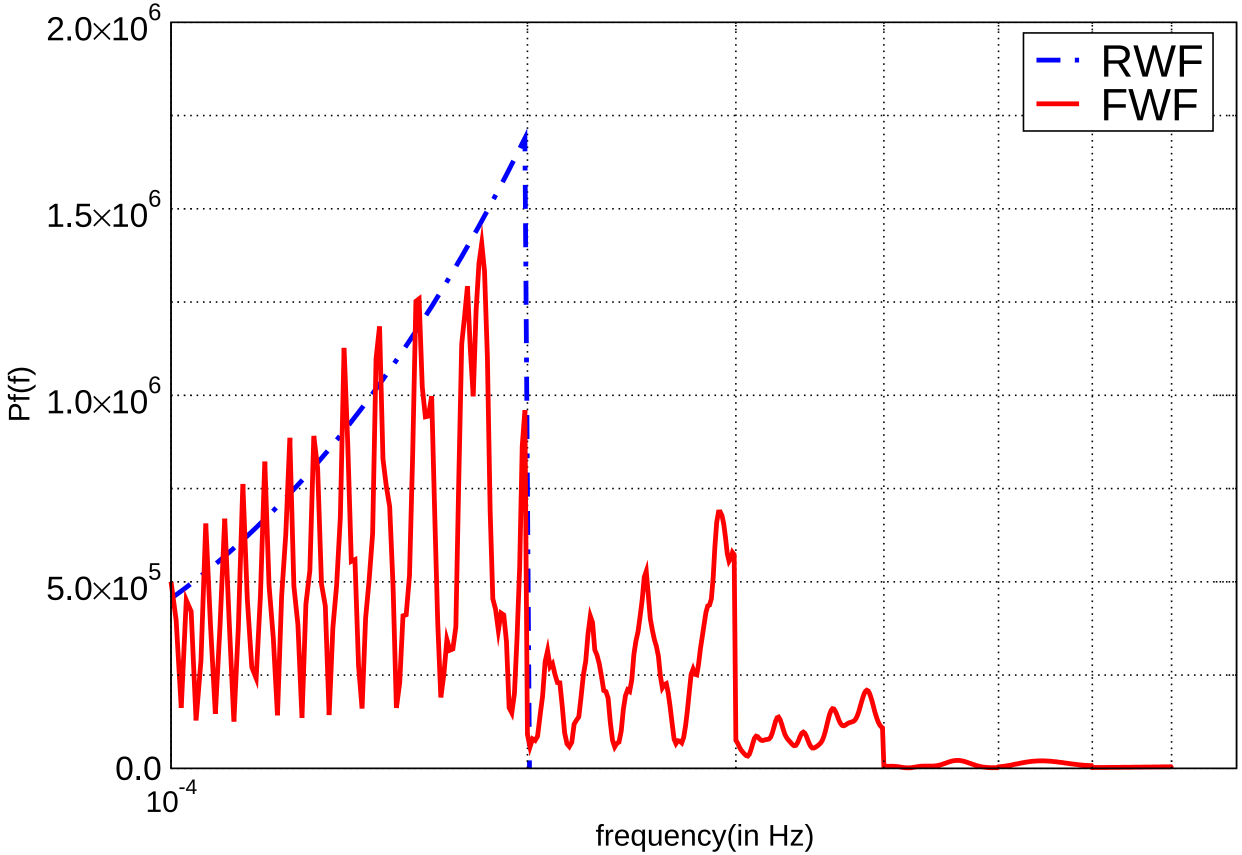

The source is assumed to be at 3 Gpc and its orientation wrt the solar-system barycentre is chosen to be $\theta_S = \cos^{-1}(-0.6)$, $\phi_S = 1$, $\theta_L = \cos^{-1}(0.2)$, $\phi_L = 3$. The spectrum is much more complicated and highly oscillatory for the FWF than for the RWF, because of interference between various harmonics. The higher frequency reach of the FWF is due to presence of higher harmonics.

Observed signal spectrum with LISA

- As for ground-based detectors Van den Broeck and Sengupta, spectrum due to the FWF has a lot more structure and is highly oscillatory because of interference between various harmonics.
- For $(10^5, 10^6)M_\odot$ system, the mass being low, the second harmonic and hence the RWF extends up to frequencies $\sim 2 \times 10^{-3}$ Hz, where LISA is most sensitive. This leads to a rapid increase in the observed spectrum in this frequency region. The spectrum due to the FWF, containing higher harmonics continue beyond the RWF into the most sensitive part of the LISA band.
- For the $2(10^6, 10^7)M_\odot$ system, the frequency span of the second harmonic is small and the sensitive region of the LISA band lies beyond its maximum reach.

Observed signal spectrum with LISA

PN order	SNR	
	$(10^6 - 10^7)M_\odot$	$5.5 \times (10^6 - 10^7)M_\odot$
0	924.48	0
0.5	1025.8	211.98
1	928.48	343.17
1.5	869.78	319.34
2	824.65	266.65
2.5	809.51	277.34

SNRs due to successive PN amplitude-corrected waveforms, with phase corrections to 3.5 PN order in all cases. The orientation of the source with respect to the solar-system barycentre is chosen to be $\theta_S = \cos^{-1}(-0.6)$, $\phi_S = 1$, $\theta_L = \cos^{-1}(0.2)$, $\phi_L = 3$. For the $(10^6 - 10^7)M_\odot$ binary system, all harmonics enter deep into the sensitive part of the LISA bandwidth. Apart from an increase at 0.5PN, we see a consistent reduction in the SNR on inclusion of higher PN order amplitude corrections. or the $(5.5 \times 10^6, 5.5 \times 10^7)M_\odot$ binary system, the second harmonic fails to enter the LISA bandwidth, while the third harmonic spans a small insensitive region. Thus the SNR due to the RWF is zero, while the SNR due to the 0.5PN waveform is smaller than the SNRs due to higher order PN terms. Both sources are at a distance of 3 Gpc.

The effect of higher harmonics

- We classify sources into two types:
  Sources for which the dominant (second) harmonic has a large frequency span in the LISA band
  Sources whose dominant harmonic *fails* to enter the LISA bandwidth but the higher harmonics *do*.
- Since the upper cut-off frequency for each harmonic is inversely proportional to the total mass sources of the first type will have total mass less than some critical mass, while the second type will have masses greater than or equal to that critical mass.
- Condition that the upper cut-off of the dominant harmonic is less than or equal to the lower cut-off of LISA (i.e., by the inequality $2\,F_{\rm LSO} \leq f_{\rm s}$) determines the mass-reach of the RWF and its value is $4.39 \times 10^7 M_\odot$ (for $f_s = 10^{-4}$ Hz).

SNR versus Total Mass for Mass Ratios .1 and .01

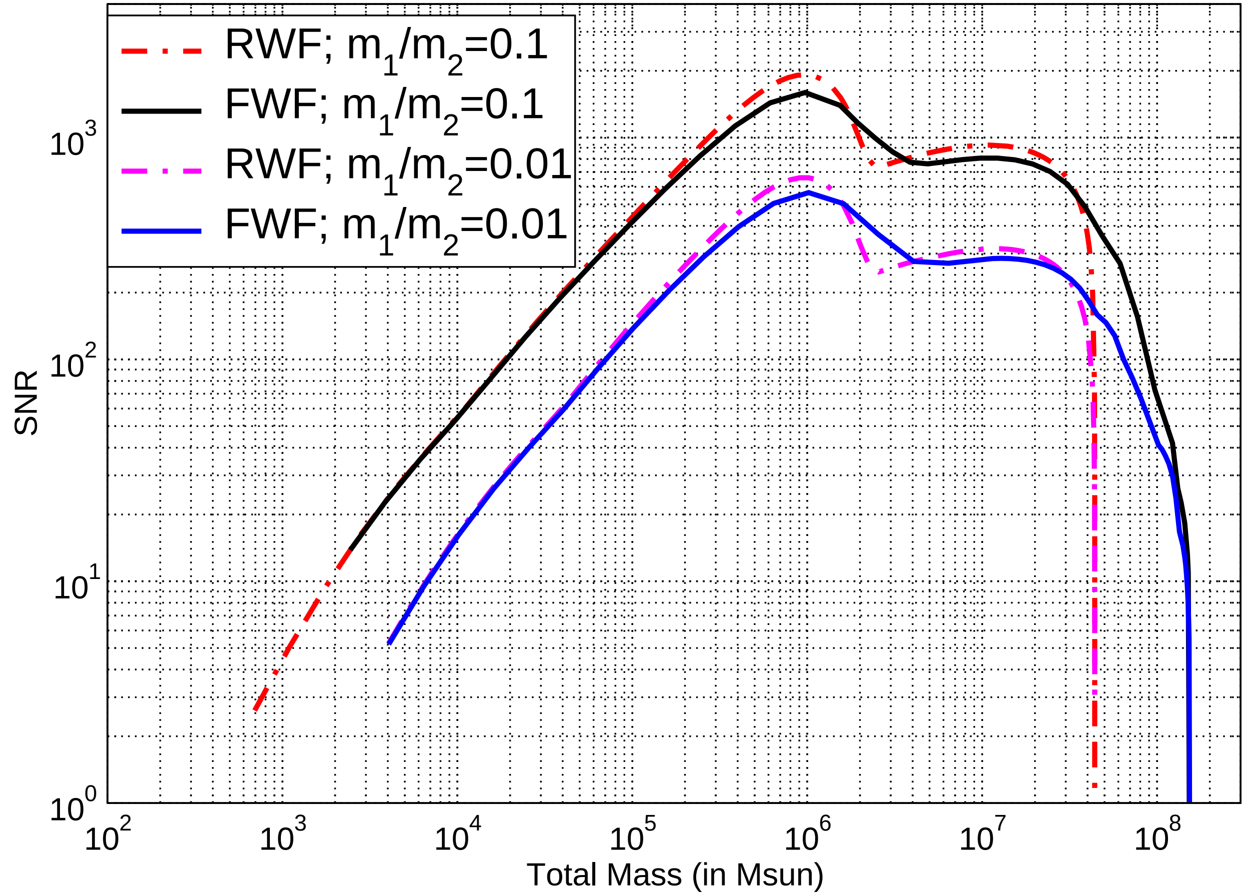

Apart from the dips due to white-dwarf confusion noise, for mass values where the RWF enters the LISA band, the SNR for RWF is more than the SNR for the FWF. For mass values where the second harmonic terminates before it reaches the LISA bandwidth, the FWF which has higher harmonics that enter the LISA band produces significant SNRs. Mass reach of the FWF is independent of the mass-ratio. For more asymmetric systems, the magnitude of the SNR is low for all masses both for the RWF and the FWF. Sources are at a luminosity distance of 3 Gpc with fixed angles given by $\theta_S = \cos^{-1}(-0.6), \phi_S = 1, \theta_L = \cos^{-1}(0.2), \phi_L = 3.$

Visibility of systems with $\mathbf{M > 4 \times 10^7 M_\odot}$

- Van Den Broeck and Sengupta pointed out an interesting effect due to higher harmonics in the FWF for ground-based detectors
- An analogous effect is found in the case of LISA in spite of the additional amplitude and Doppler modulations that exist in this case.
- Normally, the harmonic at twice the orbital frequency dominates the SNR. However, when the dominant harmonic fails to reach the LISA band the higher harmonics become important, which transpires for masses greater than $4 \times 10^7 M_\odot$.
- Even though the second harmonic falls below the lower cut-off $f_{\rm s}$ of the LISA bandwidth, the kth harmonic, $k > 2$, that has power up to a frequency $k\,F_{\rm LSO}$, might cross $f_{\rm s}$ and produce a significant SNR. Of course, the kth harmonic would fall below the LISA sensitivity band for masses which satisfy the equality $f_{\rm s} = k\,F_{\rm LSO}$. Thus, higher PN order waveforms, which bring in higher harmonics, are capable of producing a significant SNR, even when the RWF fails to produce any.

SNR versus Total Mass for Diff PN Orders

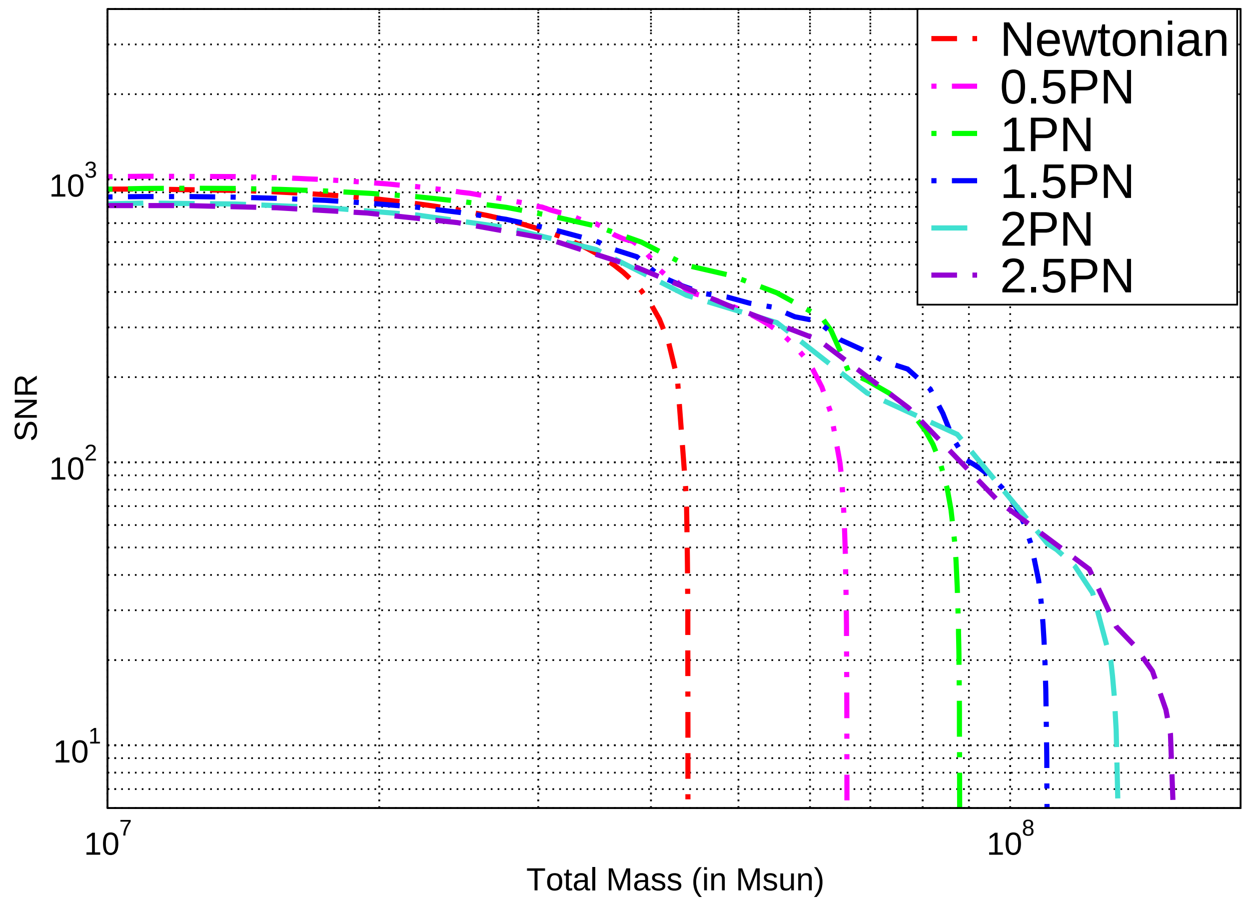

3.5PN phasing and mass-ratio of 0.1 - The $(2n+2)^{\mathrm{th}}$ harmonic first appears at the nth PN order. Upper cut-off of the k^{th}-harmonic of the orbital frequency in the frequency domain is proportional to k and inversely proportional to the total mass. As the mass increases the upper cut-off for the 2^{nd} harmonic falls below the lower cut-off of the LISA detector, leading to a zero value of SNR due to the RWF. The higher harmonics still enter the sensitive bandwidth of LISA and higher PN order waveforms produce significant SNR. The 2.5PN waveform has the highest mass-reach, being 3.5 times the mass-reach of the RWF.

Visibility of systems with $\mathbf{M > 4 \times 10^7 M_\odot}$

- Thus, the use of the FWF will enable LISA to make observations of SMBHs in the astrophysically interesting mass-regime, which would not be possible had one used only the standard RWF.
- Using the expression for $F_{\rm LSO}$, the mass reach for the 2.5PN FWF, which has the seventh harmonic of the orbital frequency, is $7/2$ times the RWF (around $1.5 \times 10^8 M_\odot$). The above ratio, of course, depends on the assumption that the Schwarzschild (test particle case) LSO frequency will not be very different from the LSO frequency in the comparable mass case.
- In contrast to asymmetric systems, for systems of equal mass *all* odd harmonics are absent. For symmetric systems the mass-reach of the 2.5PN FWF will be only 3 times the mass-reach of the RWF. The 0.5PN and the 0PN, or RWF, are identical, as are the 1PN and 1.5PN waveforms.
- Decrease in SNR for the higher PN order waveforms with increasing total mass is more pronounced than in the unequal-mass case.
- Computation of the 3PN GW polarization which will introduce an harmonic at 8Ψ will be quantitatively more significant for the equal mass case as the mass reach will be better by 33% relative to the 2.5PN FWF as opposed to the unequal mass case where it is only 14%! Motivation for work in progress towards the computation of the 3PN accurate GW polarizations.

SNR versus Total Mass for Diff PN Orders

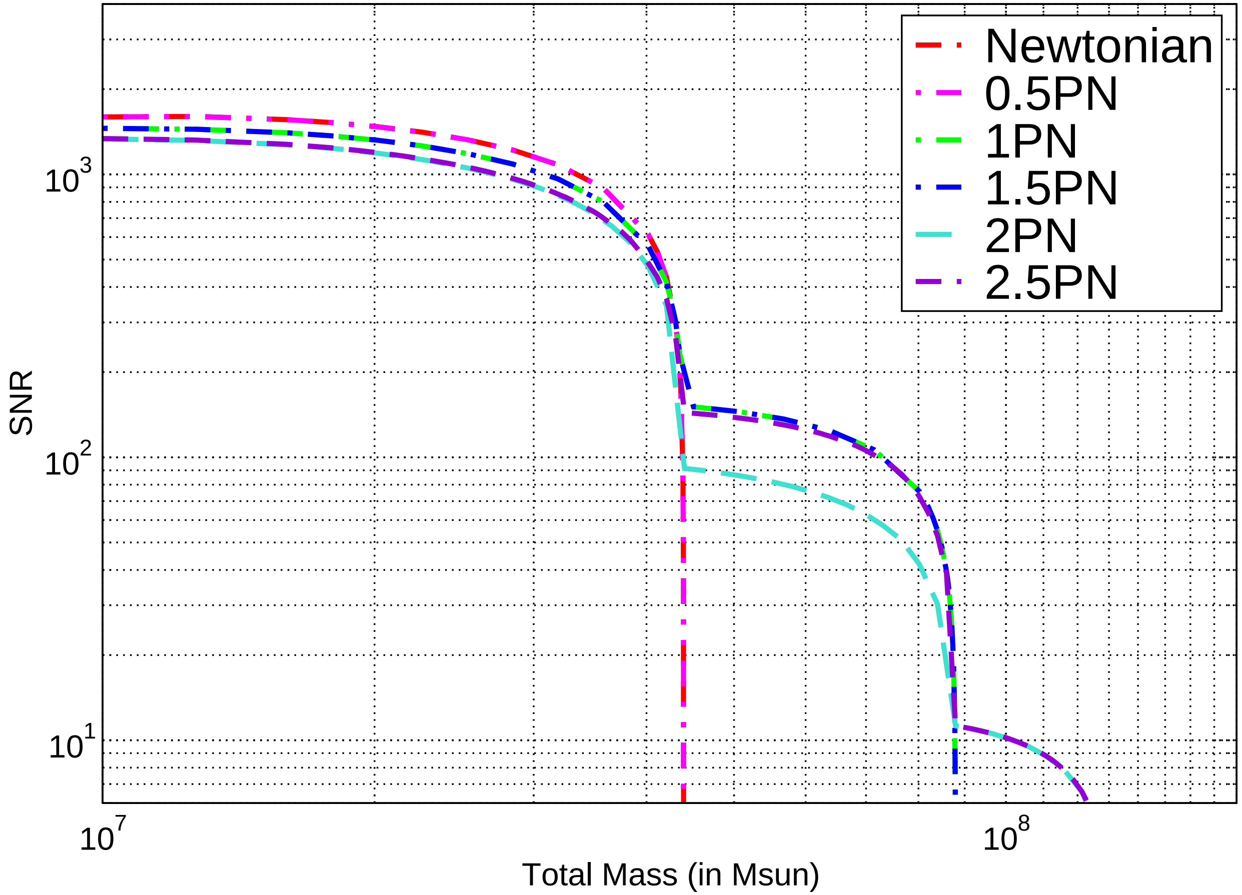

3.5PN phasing and mass-ratio of 1 - In the equal mass case, the differences in harmonic content of different PN order waveforms are more pronounced, as odd harmonics are absent. Sources are at a luminosity distance of 3 Gpc with fixed angles given by $\theta_S = \cos^{-1}(-0.6), \phi_S = 1, \theta_L = \cos^{-1}(0.2), \phi_L = 3$.

Distance reach with the 2.5PN FWF

- We compare the distance-reach of the RWF and the 2.5PN FWF.
- Results shown graphically in next Fig and are similar in appearance to the mass-reach plot.
- The mass-reach of the RWF is $\simeq 4 \times 10^7 M_\odot$. For a system of total mass $5 \times 10^7 M_\odot$, the plot shows that LISA can detect such binaries with an SNR of 10 at a luminosity distance of 100 Gpc ($z \simeq 15$).
- SMBHs of total mass $\sim 10^8 M_\odot$, not even observable using RWF templates, have a distance-reach as high as 10 Gpc ($z \simeq 1.5$) with an SNR of 10.
- Proposals to extend the frequency band-width of LISA up to 10^{-5} Hz have been discussed. Then FWF can increase the mass-reach of LISA to even around $10^9 M_\odot$.
- LISA can then observe a $10^9 M_\odot$ system with an SNR of about 30 at 3 Gpc, if it uses templates based on the 2.5PN FWF for data-analysis.

Luminosity distance vs Total Mass for SNR=10

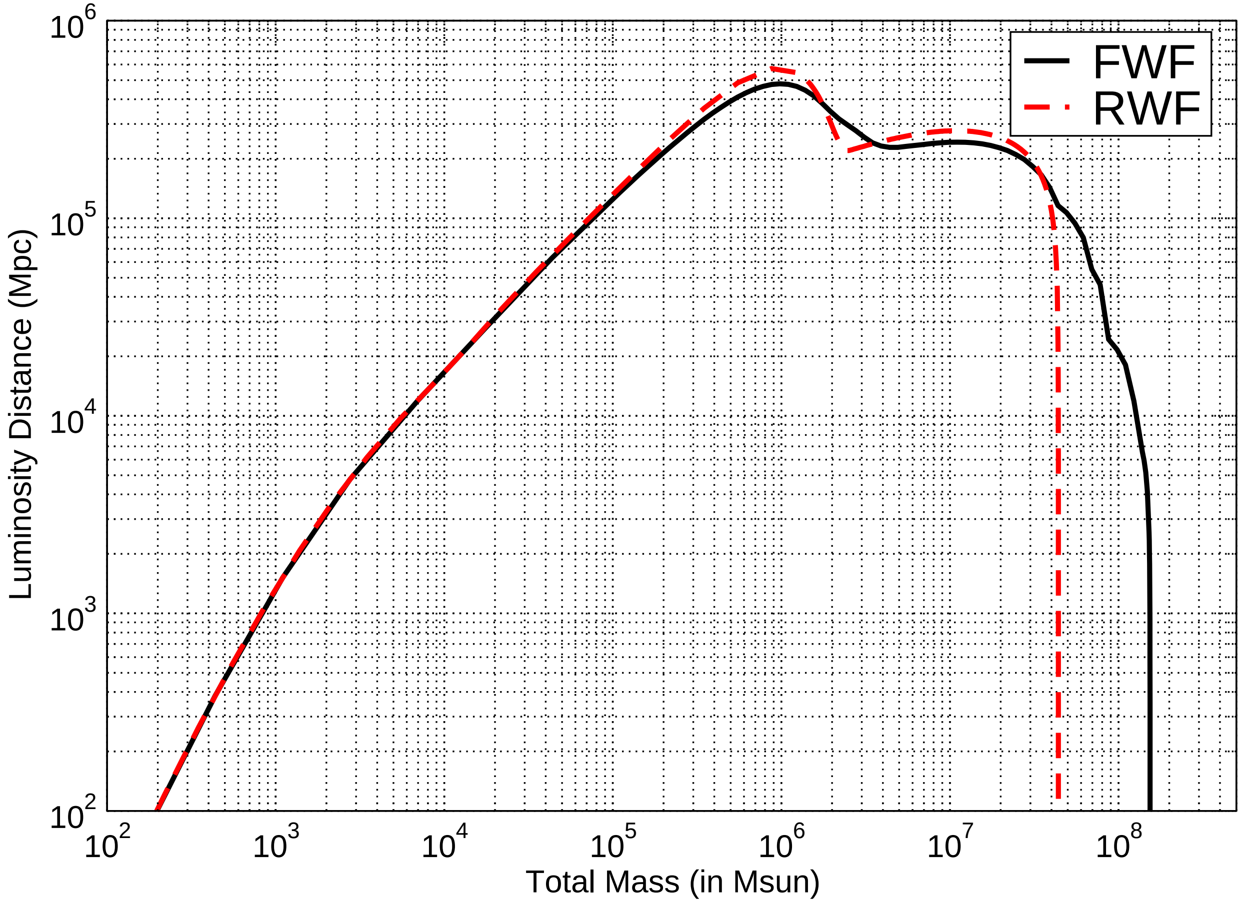

The systems have mass-ratio of 0.1. The distance reach can be as large as 500 Gpc for systems where the second harmonic enters the LISA bandwidth. Systems undetectable by the RWF (of mass around $10^8 M_\odot$) can be detected by the FWF at distances up to 10 Gpc. The location and orientation of the sources are the same as in the earlier figures.

Sensitivity of SNR to location and orientation

- All the results for SNR using the amplitude-corrected waveforms quoted earlier have been for a fixed choice of location and orientation of the source (defined by the angles($\theta_S, \, \phi_S, \, \theta_L, \, \phi_L$)) wrt the barycentre coordinate system.
- To conclude we look into the variation in the value of SNR for sources at various locations in the sky and various orientations.
- We consider a collection of sources randomly oriented in the sky and study the probability distribution of their SNRs. The results of our simulations (consisting of 8000 random realisations of the angles involved) are shown in Figs.
- We see that the most probable SNR due to the FWF for a $(10^5, \, 10^6)M_\odot$ binary is less than the most probable SNR due to the RWF, indicating that this trend is independent of the source location and orientation.
- A binary of mass $2 \times (10^6, \, 10^7)M_\odot$, which is undetectable by the RWF, can be observed by the FWF with a most-probable SNR of around 220.

Distribution of SNR

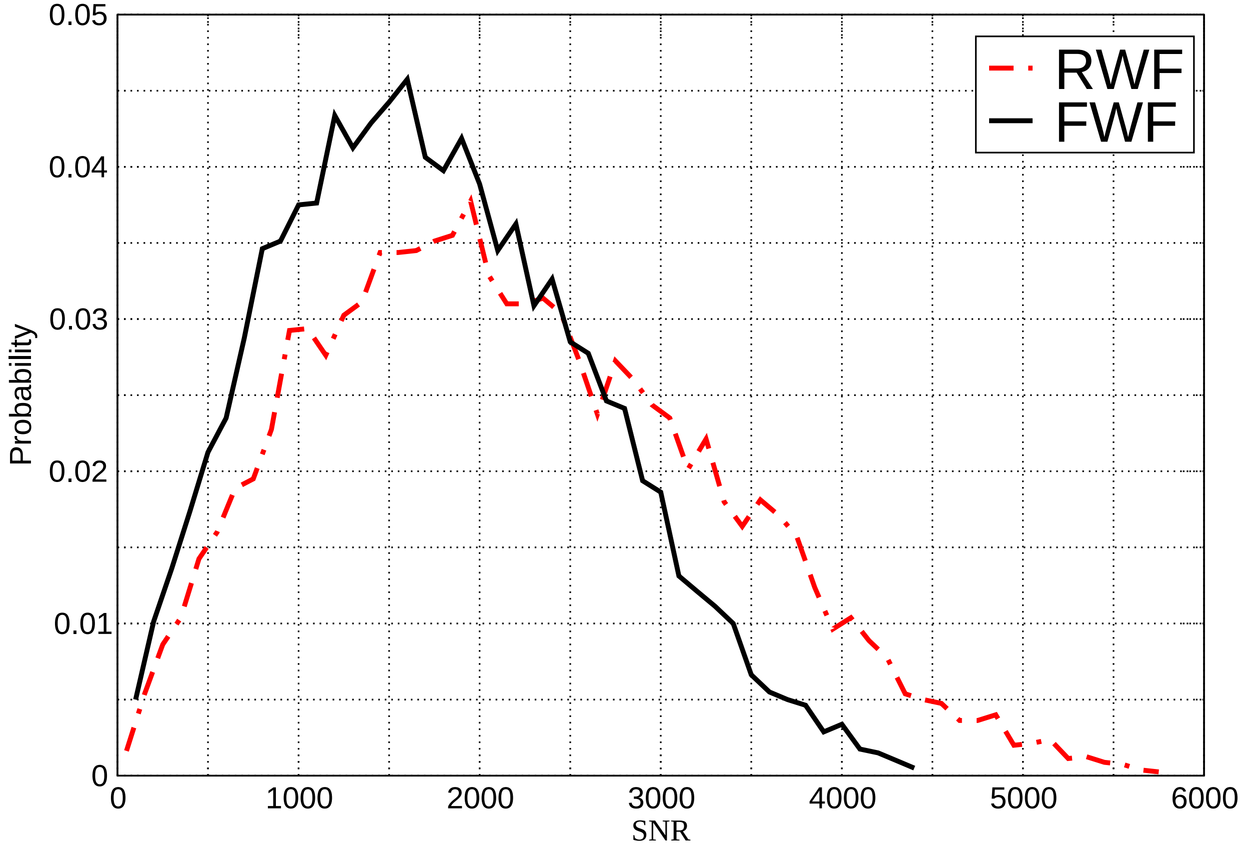

Figure plots SNRs due to both RWF and FWF for a binary of mass $(10^5 - 10^6)\, M_\odot$ randomly located and oriented.

For this mass, the most probable SNR for the FWF is lower than the most probable SNR for the RWF, like the trend shown in Table

Distribution of SNR

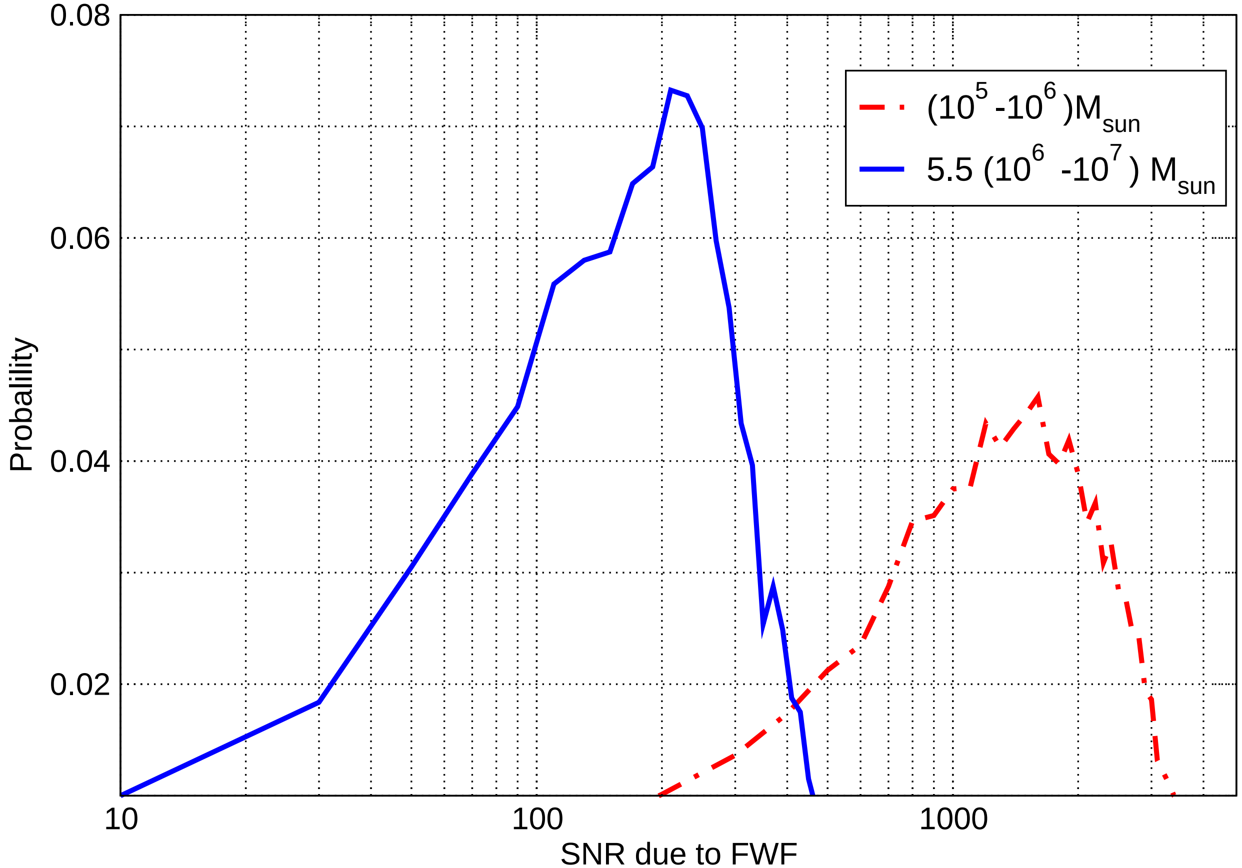

The Figure compares the SNRs due to the FWF for binaries of mass $(10^5 - 10^6)M_\odot$ and $5.5(10^6 - 10^7)M_\odot$ with sources randomly located and oriented

Concluding Remarks

- Implications of amplitude corrected 2.5PN *full* waveforms (FWF) for the construction of detection templates for LISA are investigated
- With the FWF, LISA can observe sources which are favoured by astronomical observations, but not observable with restricted waveforms (RWF). This includes binaries in the mass range $10^8 - 10^9 M_\odot$, depending on whether the lower cut-off for LISA is chosen to be at 10^{-4} Hz or 10^{-5} Hz. With an SNR of 10, these systems can be observed up to a redshift of about 1.5.
- Computation of the 3PN polarization, which will introduce an harmonic at 8Ψ (i.e. four times the dominant harmonic), in addition to the existing harmonics, could enhance the mass reach for equal mass binaries by 33% and unequal mass binaries by 14.3%.
- Implication of the FWF for parameter estimation will be far more important than the extension of LISA's mass-reach reported here. From the work of Van Den Broeck and Sengupta in the context of ground-based detectors it is clear that most parameters will be estimated with errors $\sim$ ten times smaller as compared to RWF.

Concluding Remarks

- Raises the interesting possibility that binary SMBH coalescences might be located on the sky with accuracies good enough for optical observations to identify the galaxy cluster and measure its red-shift. This improved estimation of source properites will have important consequences in shedding light on the dark energy, better understanding of SMBH formation and evolution, structure formation, etc., and is currently under investigation.
- Confined ourselves to only non-spinning black-holes ignoring the effect of spin-orbit coupling at 1.5PN and 2.5PN and spin-spin effect at 2PN order. The effect of spin is expected to be astrophysically significant and it is important to revisit the present analysis including spin. GW polarisations including spin would be required. More complicated due to modulations arising from spin-orbit and spin-spin couplings.
- Restricted to the inspiral phase and used a physical picture of the LSO that is based on the test-particle limit. For comparable masses, the notion of LSO is not as sharp, or unique, and hence our results are probably idealized limits of the real situation. Recent Numerical relativity results for late inspiral and merger should allow one to compare the results of numerical templates with those studied here to provide a better understanding of how higher harmonics facilitate the mass reach of our detectors.

How higher harmonics affect signal visibility

- Reduction in SNR at higher PN orders can be understood by studying the structure of $|\tilde{h}(f)|^2$, the numerator in the integrand of the SNR. There are basically three types of terms:
    1. *Direct* terms in which the phases in Eq. cancel

$$A^2_{(k,n/2)}(t(f/k))\, f^{-\frac{7}{3}}\, (Mf)^{\frac{2n}{3}},$$

    2. *Interference* terms between *different* PN corrections of the *same* harmonic,

$$A_{(k,m/2)}(t(f/k))\, A_{(k,n/2)}(t(f/k))\, f^{-\frac{7}{3}}\, (Mf)^{\frac{m+n}{3}}\, \cos[\phi_{(k,m/2)}(t(f/k)) - \phi_{(k,n/2)}(t(f/$$

    3. *Harmonic mixtures* which are terms containing the interference between *different* PN corrections of *different* harmonics, e.g. the $m/2^{\rm th}$ PN correction of the $k^{\rm th}$ harmonic and $n/2^{\rm th}$ PN correction of the $l^{\rm th}$ harmonic.

$$A_{(k,m/2)}(t(f/k))\, A_{(l,n/2)}(t(f/l))\, f^{-\frac{7}{3}}\, (Mf)^{\frac{m+n}{3}}\, \cos[\psi(t(f/k)) - \phi_{(k,m/2)}(t(f/k)) - \psi($$

- All these terms are scaled by $\mathcal{M}^{5/3}$,

Higher harmonics in ground-based detectors

- For ground-based detectors a similar effect was found by Van den Broeck and Sengupta for a different but corresponding mass region.
- The lower cut-off for a typical ground-based detector, say Advanced LIGO is 20Hz, and the effect of higher harmonics is seen for masses less than $\sim 220 M_\odot$.
- Polarisation amplitudes and phases are constants. The RWF contains only the Newtonian term of the second harmonic and thus $|\tilde{h}(f)|^2$ consists of a single direct term with $n = 0$ and $k = 2$.
- With the inclusion of higher-order amplitude terms in the waveform, PN corrections to the dominant harmonic, and higher harmonics and their PN corrections also contribute to the SNR.
- Signal power spectrum $|\tilde{h}(f)|^2$ will contain all three types of terms.
- From the form of the *direct terms*, their contribution to the SNR will be positive definite. For ground-based detectors, the frequency dependence of the *direct* and *interference* terms will just be a power law. Sign of the interference terms (and consequently their contribution to the SNR) depends on the difference between the polarisation phases of different PN corrections for the same harmonic.

Higher harmonics in ground-based detectors

- Van Den Broeck and Sengupta showed that for a given harmonic, for all allowed values of the parameters $(\nu, \theta, \phi, \psi, i)$, each PN correction is almost "out of phase" with *both* the PN correction preceding and succeeding it. The resulting negative terms (representing destructive interferences) reduce the SNR as one includes higher PN amplitude corrections in the waveform.
- Third type of terms, harmonic mixtures, are highly oscillatory functions of the frequency, as the phase difference $\psi(t(f/k)) - \psi(t(f/l))$ between the $k^{\rm th}$ and the $l^{\rm th}$ harmonic become even or odd multiples of π. As one integrates over f, these oscillations tend to cancel out, and thus the contribution to the SNR from these terms are numerically much smaller relative to the first two types of terms

Higher harmonics in LISA - $\mathbf{M < 4 \times 10^7 M_\odot}$

- For LISA, because of the polarisation factors, amplitudes of none of the three types of terms is a simple power-law in f.
- Periodic variation of, $A_{(2,0)}$ (period being one year) appears as an amplitude modulation $A_{(2,0)}(t(f/2))$ in the FT, where the argument $t(f/2)$ of $A_{2,0}$ is given by

$$t(f/2) = -\frac{5}{256\pi^{8/3}\mathcal{M}^{5/3}}\frac{1}{f^{8/3}} + \text{PN corrections}.$$

- In the FD $A_{(2,0)}$ will undergo one complete oscillation as f varies from $2F_{\rm in}$ to $2F_{\rm LSO}$. However, because of the *inverse* power-law dependence on f, the oscillation of $A_{(2,0)}$ is confined to a small frequency interval above $F_{\rm in}$ and remains fairly constant over a major portion of the frequency span $2(F_{\rm LSO} - F_{\rm in})$.
- For masses higher than the one shown in Fig, this region of significant variation moves to the left of the figure. On including in our analysis the effect of detector sensitivity (weighting down by $S_h(f)$) this variation of $A_{(2,0)}$ gets damped out when one evaluates the integral. For masses satisfying $2F_{\rm in} \ll 10^{-4}$ Hz, the lower cut-off for LISA, this region of variation will fall below the LISA band.

Variation of Polarisation Amplitude of RWF

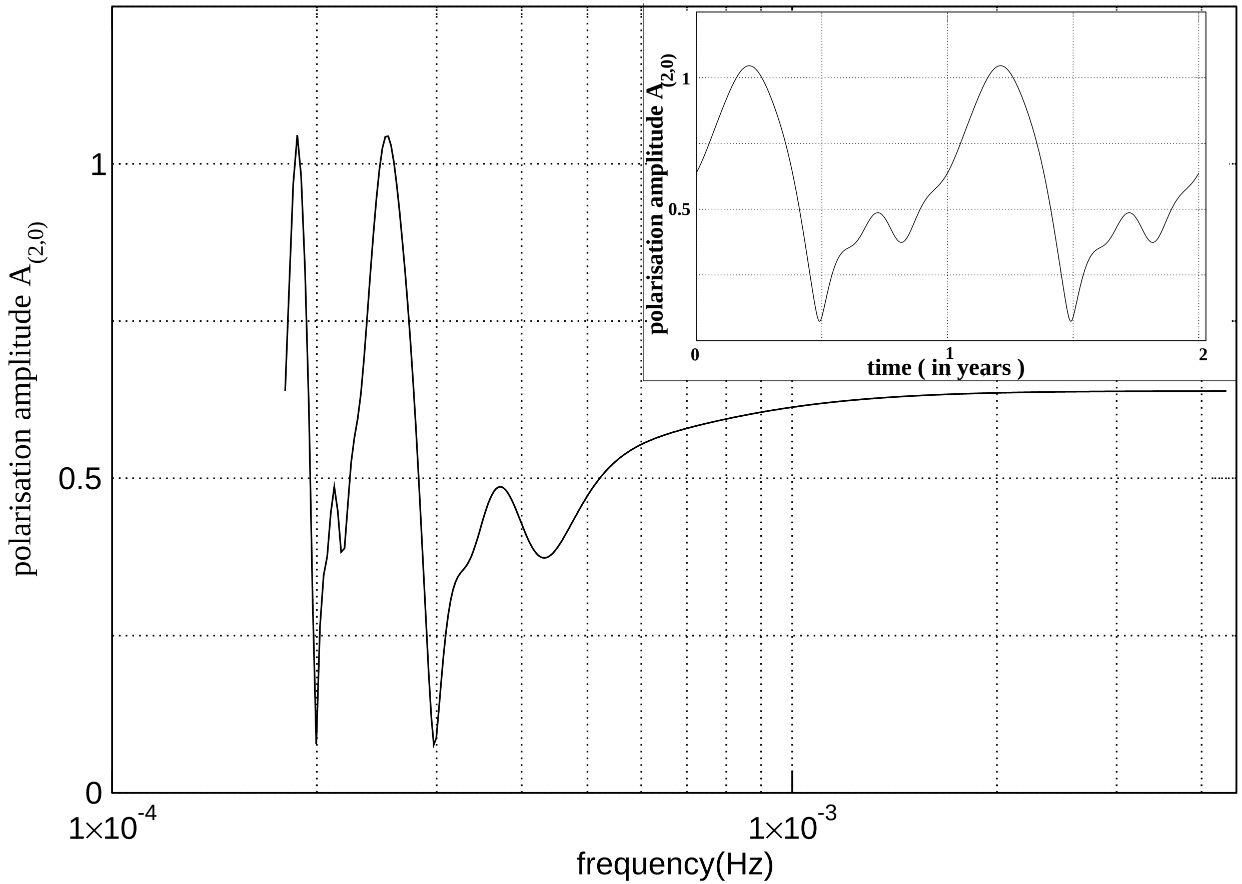

Variation of polarisation amplitude of the RWF with frequency and time (inset). The inset, plotted over a duration of two years clearly shows periodicity due to LISA's orbital motion around the Sun. The binary mass, $(10^6 - 10^4)\,M_\odot$, has been chosen such that it can, in principle, be observed for two years. The plot in the frequency domain shows that the variation of the polarisation amplitude is confined to a very small part of the frequency span of the dominant harmonic, and essentially behaves as a constant in the frequency domain.

Higher harmonics in LISA - $\mathbf{M < 4 \times 10^7 M_\odot}$

- Polarisation phases determining the sign of the interference terms between the same harmonics also vary with f. However, phase relationships of the polarisation phases are independent of the parameter values. Thus the modulations which change the values of (θ, ϕ, ψ, i) do not affect the trend of reduction of SNR with amplitude corrections. The Doppler modulations, which appear in only harmonic mixtures, are also not important as far as SNR is concerned.
- As the difference between the polarisation phases of successive PN corrections of the same harmonic tend to be nearly π, alternate PN corrections necessarily interfere constructively leading to positive contributions also from the interference terms.
- Numerical value of the contribution to SNR from each of these terms depends on the magnitude of the polarisation amplitude and the power of (Mf). Numerical values of contributions from interference between higher PN corrections of the second harmonic successively decrease. Thus, inclusion of amplitude corrections will lead to an overall reduction in SNR.